 ICCES, vol.9, no.4, pp.225-231

BIE-based aeroacoustic design procedure

R.M.A. Marretta[1], C. Orlando[1], M. Carley[2]

Summary

A propeller low noise design procedure based on boundary integral equation is presented. The aerodynamic field is computed via a potential-based boundary element method for lifting body while the aeroacoustic emitted field is calculated on the basis of the Ffowcs Williams-Hawkings equation. Families of airfoils sections are aerodynamically processed to select the ones that meet the requested performance. Successively, the airfoil sections characterized by the lowest noise emission, among the previously selected ones, are chosen to built the propeller blade. Eventually the whole propeller aeroacoustic performances are analyzed.

Introduction

The aeronautical propeller design problem is a multidisciplinary problem involving aerodynamic, structural and acoustic analyses. Due to the increase of modern turbo-prop engines efficiency, the use of propeller based engine has became more attractive for a wide range of air transport systems, in particular for the regional transport aircraft operating in the subsonic regime. Even though aerodynamic efficiency is the prime objective of an aeronautical propeller design and structural quality is mandatory, acoustic optimization has also become an economical issue because of the airport taxes related to the acoustic quality of the aircraft. The problem of noise generated by a propeller operating in mean flow, whether isolated or installed [1], is quite well understood, but the integration of acoustic criteria in propeller design remain an interesting research topic. Numerical analyses have pointed out the main factors affecting aerodynamic propeller performances [2-5] and several methods have been developed to study the aeroacoustic problem [6-8]. In this paper a low noise propeller design procedure is presented. By using a BEM code for aerodynamic calculations and a noise prediction method, a blade geometry able to fulfill the required propeller operating conditions taking into account the noise emitted by the system is generated. A database of airfoils families is used in conjunction with the BEM and the aeroacoustic computation method to adaptively generate the blade geometry which has *i*) the required radial distribution of circulation, to ensure aerodynamic efficiency, *ii*) the requested chord radial variation, to ensure structural safety, and *iii*) the lowest noise emission level.

Aerodynamic Field Computation

The first step of an aeroacoustic computation is the determination of the aerodynamic field around the emitting body in terms of pressure and velocity distribution. To analyze the aerodynamic field around a propeller blade a BEM code based

[1]Dipartimento di Tecnologie ed Infrastrutture Aeronautiche, Universitá di Palermo, Italy
[2]Department of Mechanical Engineering, University of Bath, UK

on the boundary integral formulation for the potential flow around lifting body is used. Under the assumptions of quasi-steady, inviscid, incompressible and attached flow problem, the aerodynamic field for lifting body is represented by the following boundary integral equation [9]

$$c\phi = \int\limits_{\partial\Omega_b} \left(\phi \frac{\partial G}{\partial n} - G \frac{\partial \phi}{\partial n} \right) d\partial\Omega + \int\limits_{\partial\Omega_w} \Delta\phi \frac{\partial G}{\partial n} d\partial\Omega \tag{1}$$

where ϕ is the velocity potential, G is the fundamental solution of the Laplace equation [10], c is a coefficient defined as in [11], $\partial/\partial n$ represents the derivative along the body surface normal direction, $\partial\Omega_b$ is the body boundary, $\partial\Omega_w$ is the wake boundary and $\Delta\phi$ is the potential jump across the wake surface. The solution ϕ is assumed to be given by the linear combination of the particular solution ϕ_R related to non-lifting problem with asymptotic velocity U_∞ and of the non-trivial solution ϕ_A associated with lifting body in absence of asymptotic stream. By so doing the following integral equations, with the relative boundary conditions obtained by considering the body as rigid and impermeable, stand

$$c\phi_R = \int\limits_{\partial\Omega_b} \left(\phi_R \frac{\partial G}{\partial n} - G \frac{\partial \phi_R}{\partial n} \right) d\partial\Omega \qquad \text{on } \Omega, \qquad \frac{\partial \phi_R}{\partial n} = \frac{1}{U_\infty} \frac{\partial \phi}{\partial n} \quad \text{on } \partial\Omega. \tag{2}$$

$$c\phi_A = \int\limits_{\partial\Omega_b} \phi_A \frac{\partial G}{\partial n} d\partial\Omega + \int\limits_{\partial\Omega_w} \Delta\phi \frac{\partial G}{\partial n} d\partial\Omega \qquad \text{on } \Omega, \qquad \frac{\partial \phi_A}{\partial n} = 0 \quad \text{on } \partial\Omega. \tag{3}$$

Both the problem are solved numerically by using the boundary element method as described in [9, 11]. Once the velocity potential distribution on the boundary, i.e. along the airfoil surface, is known, the pressure distribution, in terms of pressure coefficient C_{p0} [REF], is calculated from the velocity field obtained by computing the gradient of the potential ϕ. As soon as the local Mach number M_{loc} becomes equal to the critical one, the pressure coefficient C_{p0} obtained under the incompressibility assumption, is modified as follow

$$C_p = \sqrt{\frac{1}{1 - M_{loc}^2}} C_{p\,0}. \tag{4}$$

Aeroacoustic Field Computation

Once the aerodynamic field, in terms of pressure and normal velocity distribution at the airfoil surface, is computed via the previously described boundary integral equations it is used as input for the time-domain noise prediction method developed in [12]. The solution of the acoustic wave equation is a convolution of

the source terms with the proper Green's function (more detail on the formulation are given in [12, 13]) that can be evaluated by using the distribution theory [14] to yield the solution for the loading, p'_L, and the thickness, p'_T, noise in terms of integrals over the body surface. In particular, one has

$$4\pi p'_L = \frac{1}{c_0}\int\limits_{\partial\Omega}\left[\frac{1}{1-\mathbf{M}_s\cdot\mathbf{D}}\frac{d}{d\tau}\left(\frac{\mathbf{L}\cdot\mathbf{D}}{R(1-\mathbf{M}_s\cdot\mathbf{D})}\right)-\frac{\mathbf{L}}{R(1-\mathbf{M}_s\cdot\mathbf{D})}\cdot\left(\frac{\mathbf{R}}{R}-\frac{\dot{\mathbf{R}}}{1-\mathbf{M}_s\cdot\mathbf{D}}\right)\right]d\partial\Omega \tag{5}$$

$$4\pi p'_T = \gamma\int\limits_{\partial\Omega_b}\left[\frac{1}{R(1-\mathbf{M}_s\cdot\mathbf{D})}\frac{d}{d\tau}\left(\frac{\rho_0 v_n(1-\mathbf{M}_\infty\cdot\mathbf{D})}{R(1-\mathbf{M}_s\cdot\mathbf{D})}\right)-\gamma c_0\frac{\rho_0 v_n\mathbf{M}_\infty}{R(1-\mathbf{M}_s\cdot\mathbf{D})}\cdot\left(\frac{\mathbf{R}}{R}-\frac{c_0}{\gamma}\frac{\dot{\mathbf{R}}}{1-\mathbf{M}_s\cdot\mathbf{D}}\right)\right]d\partial\Omega \tag{6}$$

where c_0 is the sound velocity, ρ_0 the air density, v_n is the velocity component normal to the boundary $\partial\Omega$, while $\mathbf{M_s}$ and $\mathbf{M}_\infty$ are the source and the free stream Mach numbers, respectively, and $\mathbf{L}$ is the pressure load force. The remaining quantities in Eq.(5) and (6) are defined as follow

$$\begin{aligned} &R=\sqrt{(1-\mathbf{M}_\infty^2)(\mathbf{x}-\mathbf{y})^2+(\mathbf{M}_\infty\cdot(\mathbf{x}-\mathbf{y}))^2}\\ &\mathbf{R}=\frac{\partial R}{\partial x_i},\quad \mathbf{D}=\frac{\mathbf{R}+\mathbf{M}_\infty}{(1-\mathbf{M}_\infty^2)},\quad \gamma^2=\frac{1}{1-|\mathbf{M}_\infty|^2}\end{aligned} \tag{7}$$

being $\mathbf{x}$ and $\mathbf{y}$ the observer and source location, respectively. It is worth noting that all quantities in square brackets in Eq.(5, 6) are calculated at the retarded time τ defined as

$$\tau = t-\frac{R+\mathbf{M}_\infty\cdot(\mathbf{x}-\mathbf{y})}{(1-\mathbf{M}_\infty^2)\,c} \tag{8}$$

Once the blade mesh, the loading and velocity distribution along with the operating conditions are known, at each time step the retarded time τ is computed using the Newton-Rhapson method and all the relevant source properties are computed. Then, the required quantities are calculated at each mesh point and the acoustic integrals are evaluated over the body (airfoil or blade) surface.

Low-noise design approach

The approach used to obtain an aeroacoustic designed propeller consists of two main steps: starting from a widespread database, called (*main airfoil database*), containing all the available airfoil geometry , a *restricted database* is first built by selecting and storing all those airfoils, and the related aerodynamic properties, that match the chosen radial blade circulation distribution to ensure the requested propeller performances. As second step, all these allowable airfoil sections are aeroacoustically processed in order to identify the particular airfoil characterized by the lowest noise emission level at a particular observation point. The propeller design parameters are the in flow mach number, the rotation speed of the propeller, the solidity, the altitude, the required traction, the propeller diameter, its number of

blades and the number of sections per blade. It is worth underlining that the blade chord radial distribution has been chosen to be an input for the proposed procedure in such a way to obtain and check the resulting propeller meets the most convenient and reliable blade geometry from industrial, manufacturing and economical points of view. Once the design parameters are set, the prescribed circulation in terms of lift coefficient distribution along the blade radial direction is calculated and the last input for the proposed aeroacoustic propeller design procedure is represented by the airfoil database containing all the available airfoil section geometry. The design procedure works as follow: for each blade radial section, namely r, the angle of attack and sweep angle are initialized,then the composed velocity, the chord value at the particular radial section and the first airfoil geometry are passed as input to the aerodynamic BEM code based on the previously described boundary integral formulation. The aerodynamic BEM analysis gives as results the local mach number distribution M_{LOC} around the airfoil boundary and the lift coefficient C_L. The BEM outputs enter into two parallel conditions check loops. The first one to check if compressibility corrections must be taken into account. The same check loop is devoted to increase the sweep angle in order to avoid extreme compressibility effect and to discard the current airfoil as ineffective if the maximum sweep angle is reached. In this case, the procedure is restarted using the next airfoil stored in the main airfoil database. The second check loop compares the lift coefficient computed by the BEM code with the requested one. If the percentage discrepancy is lower than 5%, the airfoil geometry, the aerodynamic properties and the pressure distribution around the airfoil boundary are stored in the *restricted database* and the procedure restarts analyzing the next airfoil section of the *main airfoil database*. On the other hand, if the condition on C_L is not fulfilled, the procedure increases the pitch angle and recalls the aerodynamic BEM code until the angle of attack reaches its maximum prescribed value. Even in this case the current airfoil is skipped and the procedure restarts with the next airfoil section of the *main airfoil database*.

Once all the available airfoil sections stored in the *main database* are processed, the *restricted database* becomes the input for the aero-acoustic code based on the previously described time-domain formulation. The sound pressure level SPL at prescribed observation points are computed for all the aerodynamically allowable airfoil sections and the one characterized by the lowest noise emission level is chosen as the aero-acoustic optimal profile for the blade section r and the procedure restarts for the next blade section $r+\Delta r$.

Results

The design parameters have been set using data furnished by ATR for the turboprop ATR72/500 aircraft. Three distinct flight conditions (climb at 0 ft, cruise at

17000 ft and cruise at 25000 ft and respectively referred to as $CLIMB0$, $FL170$ and $FL250$) are used to design the propeller blade. It has been assumed that the propeller has six blades, its disc and hub diameter are 3.86 m and 0.25 m, respectively and the solidity value is 0.038. The propeller pitch and pitch angle at the 75% of the blade radius for the propellers optimized in the three flight conditions are listed in Tab.1. The aeroacoustic optimized propeller traction are also shown in Tab.1 in comparison with the ATR requested values. The 6-bladed propellers, designed at the three distinct flight conditions, have also been tested in off-design flight configurations, revealing all the three propellers fulfill the requested off-design conditions.

Table 1: Computed and requested data

	$CLIMB0$	$FL170$	$FL250$
Pitch Angle	29.53°	46.3°	45.74°
Prop. Pitch	5.95	9.2	10.49
Trac. ATR	17820	10630	7480
Trac. Computed	18391	10697	7496

Once the propeller geometries are generated by using the low-noise design approach, the aeroacoustic characteristics of the three designed propellers are compared by computing the whole propeller radiated noise on two sidelines in acoustic near- and far-fields. The near-field noise is computed on a line parallel to the axis of rotation, 1.5 radii from the center of rotation while the far-field noise is computed 15 radii from the propeller axis. Acoustic results are presented in terms of near- and far-field SPL power spectrum in cruise at 25000 ft in Fig.(1) and (2), respectively. It appears that the propeller $FL250$, optimized at flight level 250, always shows the lowest sound pressure level and that the discrepancy in noise emission among the three propellers increase at high frequencies. The same stands for the propellers in cruise at 17000 ft and in climb at 0 ft.

Conclusions

A potential based boundary integral equation method for the aerodynamic and acoustic design of propellers has been presented. Three flight conditions have been chosen to design the propeller blade. Results have shown the propeller designed in cruise at 25000 ft revealed to present the lowest noise emission level in all the flight conditions, both in on- and off- design conditions.

References

1. Ardito Marretta R, Daví G, Milazzo A, Lombardi G, Carley M. (2001): "A procedure for the evaluation of installed propeller noise.", *Journal of Sound*

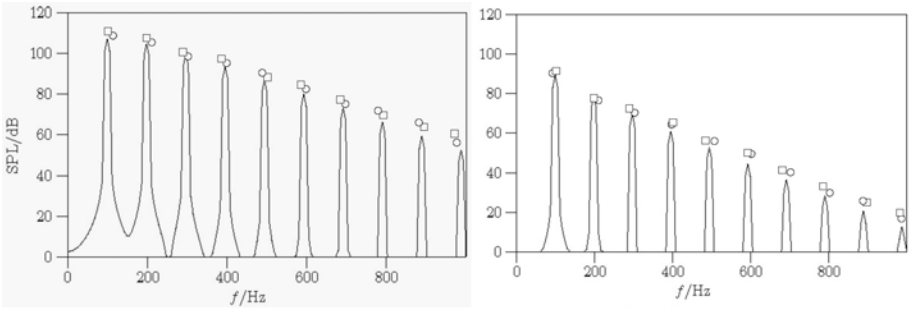

Figure 1: Near-field (left) and Far-field (right) SPL power spectrum at flight level 250. Solid line - $FL250$, open circles - $FL170$ and boxes - $CLIMB0$

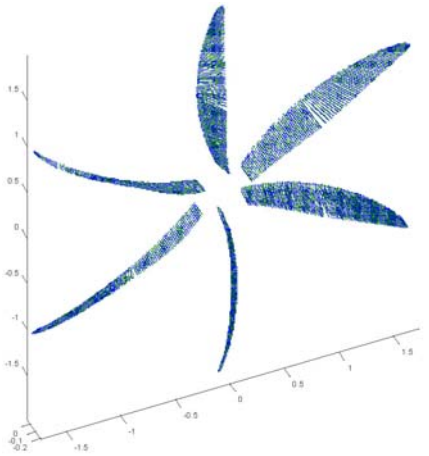

Figure 2: Aeroacoustic designed propeller

and Vibrations, Vol. 244(4), pp. 697-716.

2. Cho J, Williams MH. (1990): "Propeller-wing interaction using a frequency domain panel method.", *AIAA Journal of Aircraft*, Vol. 3, pp. 196-203.
3. Chiaramonte JY, Favier D, Maresca C, Benneceur S. (1996): "Aerodynamic interaction study of the propeller/wing different configurations.", *AIAA Journal of Aircraft*, Vol. 1, pp. 46-53.
4. Kinnas AS, Hsin CY. (1992): "Boundary element method for the analysis of the unsteady flow around extreme propeller geometries.", *AIAA Journal*, Vol. 30, pp. 688-696.
5. Graber A, Rosen A. (1987): "Velocities induced by semi-infinite helical vortex filaments.", *AIAA Journal*, Vol. 5, pp. 289-290.

6. Lighthill MJ. (1952): "On the sound generated aerodynamically. Part I. General Theory.", *Proceedings of the Royal Society (A)*, Vol. 211, pp. 564-587.
7. Ffowcs Williams JE, Hawkings DL. (1969): "Sound generation by turbulence and surfaces in arbitrary motion.", *Phil. Trans. Royal Society London (A)*, Vol. 264, pp. 342-344.
8. Farassat F. (1981): "Linear acoustic formulas for calculation of rotating blade noise.", *AIAA Journal*, Vol. 9, pp. 1122-1130.
9. Ardito Marretta RM, Daví G, Lombardi G, Milazzo A. (1999): "Hybrid numerical technique for evaluating wing aerodynamic loading with propeller interference", *Computers and Fluids*, Vol. 28, pp. 923-950.
10. Wrobel LC (2002): "The Boundary Element Method Vol. 1", Wiley.
11. Daví G, Marretta RMA, Milazzo A. (1995): "BEM formulation of the trailing edge condition" *Proceedings Of ICES '95 Symposium, Hawaii.*, Vol. 2, pp. 2933-2938.
12. Carley M, (1997): "Prediction of noise generated by a propeller in a flow" *PhD thesis*, University of Dublin, Trinity College.
13. Carley M, (1998): "SCRUMPI: Simulation code for rotation of unsteady source multi-bladed propellers at incidence" *Technical report*, Department of Mechanical Engineering, University of Dublin, Trinity College.
14. Farassat F, (1994): "Introduction to generalized functions with applications in aerodynamics and aeroacoustics" *NASA Technical Paper 3428*